Supplementary Information

Construction of 3D Pomegranate-Like $Na_3V_2(PO_4)_3$/conducting carbon composites for high power sodium ion batteries

Enhui Wang,[ab] Wei Xiang,[d] Ranjusha Rajagopalan,[ab] Zhenguo Wu,[a] Junghoon Yang[c], Mingzhe Chen,[ab] Benhe Zhong[a], Shi Xue Dou[b], Shulei Chou,[b] Xiaodong Guo,*[ab] and Yong-Mook Kang*[c]*

[a] College of Chemical Engineering, Sichuan University, Chengdu 610065, PR China

[b] Institute for Superconducting and Electronic Materials, Australian Institute for Innovative Materials, University of Wollongong, Innovation Campus, Squires Way, North Wollongong, NSW 2522, Australia

[c] Department of Energy and Materials Engineering, Dongguk University-Seoul, Seoul 04620, Republic of Korea

[d] College of Materials and Chemistry &Chemical Engineering, Chengdu University of Technology, Chengdu 610059, PR China

* Corresponding author E-mail:

Xiaodong Guo; xiaodong2009@scu.edu.cn, Shulei Chou; shulei@uow.edu.au, Yong-Mook Kang; dake1234@dongguk.edu

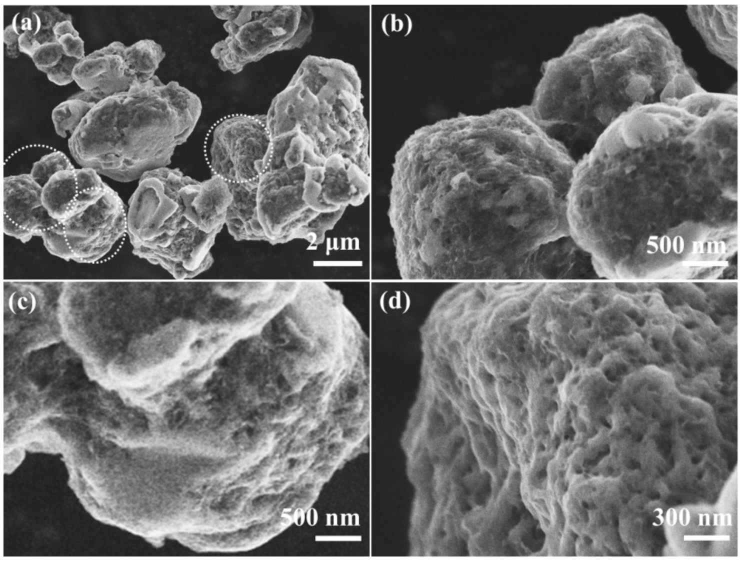

Fig. S1 SEM pictures of PL-NVP@C in (a) low magnification, and (b)(c)(d) partial enlarged images.

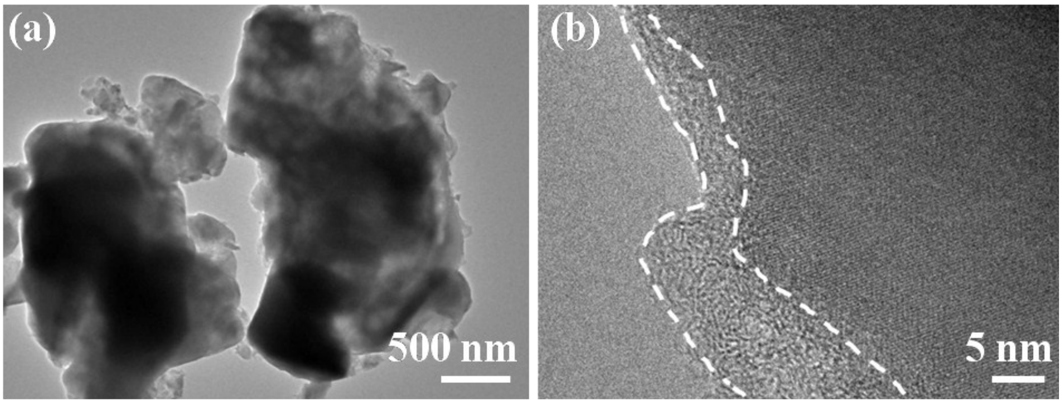

Fig. S2 TEM/HRTEM images of NVP@C.

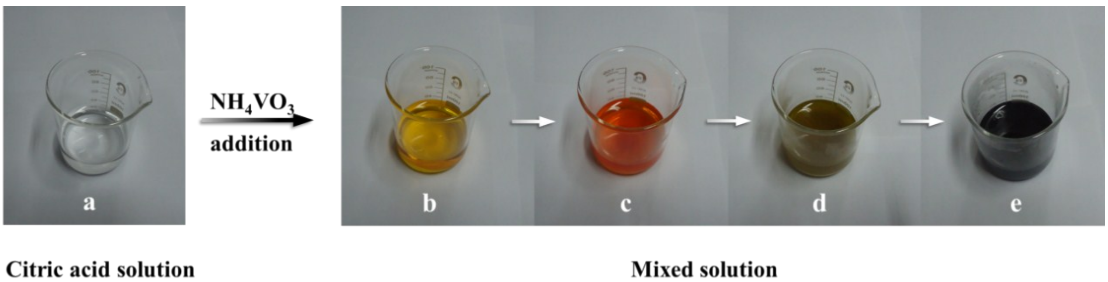

Fig. S3 The color of solution (a) before chelating process and (b)(c)(d)(e) after chelating process; (a) colorless, (b) yellow, (c) orange red, (d) green green, (e) dark bule.

(a)

$$6NH_4VO_3 + 5C_6H_8O_7 \rightarrow 6(VO)(OH)_2 + 3C_5H_6O_5 + 2C_6H_8O_7 + 3CO_2\uparrow + 6NH_3\uparrow \quad (1)$$

$$3C_5H_6O_5 + 3(VO)(OH)_2 \rightarrow 3(VO)(C_5H_4O_5) + 6H_2O \quad (2)$$

$$2C_6H_8O_7 + 3(VO)(OH)_2 \rightarrow (VO)_3(C_6H_5O_7)_2 + 6H_2O \quad (3)$$

(b)

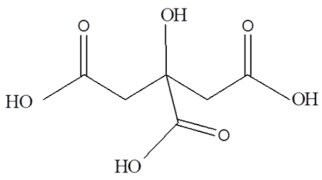

$C_6H_8O_7$

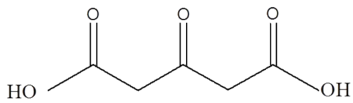

$C_5H_6O_5$

The chemical structures of $C_6H_8O_7$ and $C_5H_6O_5$.

(c)

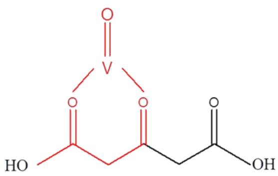

$(VO)(C_5H_4O_5)$

Possible chelating configuration between $C_5H_6O_5$ chelator and $(VO)^{2+}$.

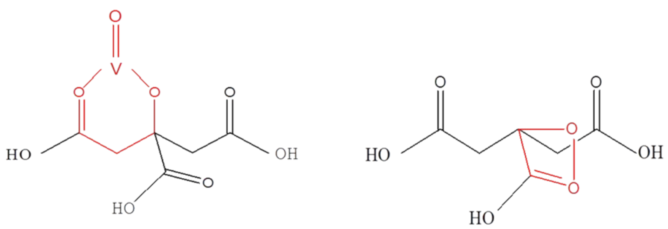

$(VO)_3(C_6H_5O_7)_2$

Possible chelating configuration between $C_6H_8O_7$ chelator and $(VO)^{2+}$.

(d)

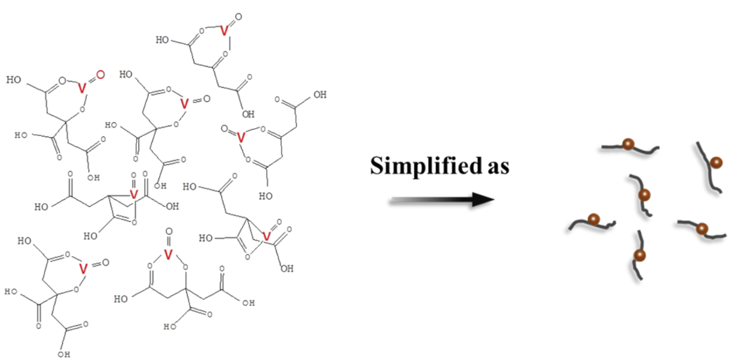

Fig. S4 (a) The corresponding reactions; (b) The chemical structures of $C_6H_8O_7$ and $C_5H_6O_5$; (c) Possible chelating configurations $C_6H_8O_7/C_5H_6O_5$ chelators and VO^{2+}; (d) The simplified chelating pattern between $C_6H_8O_7/C_5H_6O_5$ chelators and VO^{2+} when mixed together, shown in Scheme 1.

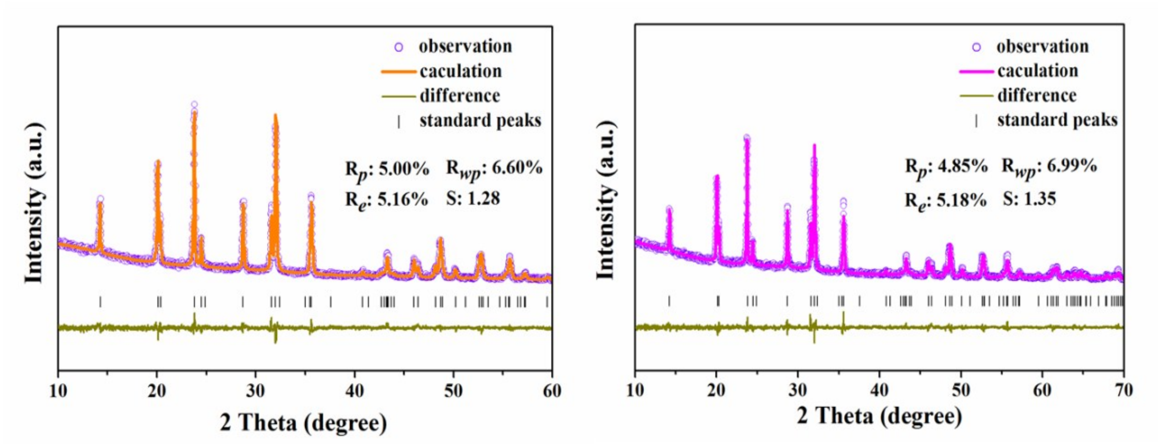

Fig. S5 Rietveld-refined XRD patterns of PL-NVP@C and NVP@C.

Table S1 Unit cell parameters of PL-NVP@C and NVP@C

Samples	a(Å)	c(Å)	V(Å^3)
PL-NVP@C	8.7259	21.8218	1438.9469
NVP@C	8.7313	21.8393	1441.8956

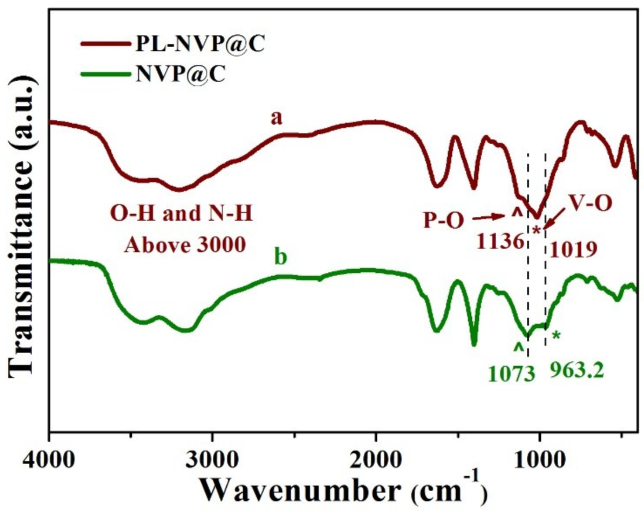

Fig. S6 FTIR spectra of (a) PL-NVP@C and (b) NVP@C.

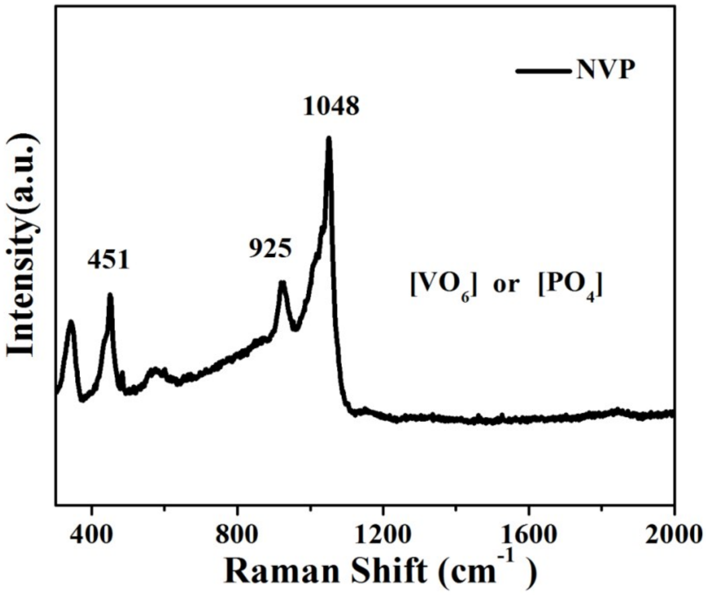

Fig. S7 Raman spectra of NVP.

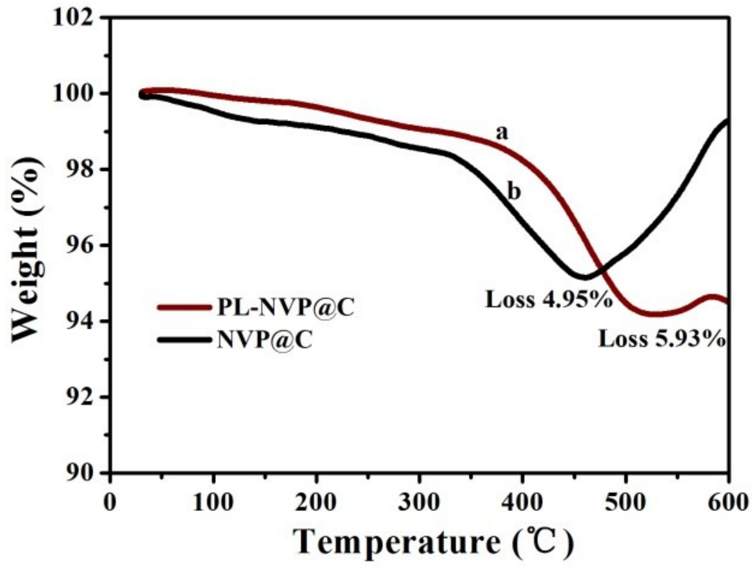

Fig. S8 Thermogravimetric curves of (a) PL-NVP@C and (b) NVP@C in the air.

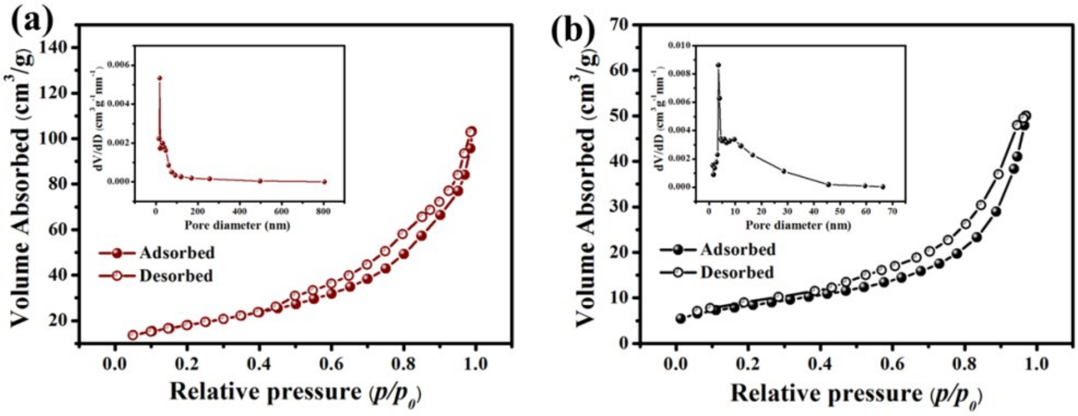

Fig. S9 Nitrogen adsorption/desorption isotherms of (a) PL-NVP@C and (b) NVP@C;

Inset: the BJH pore distribution.

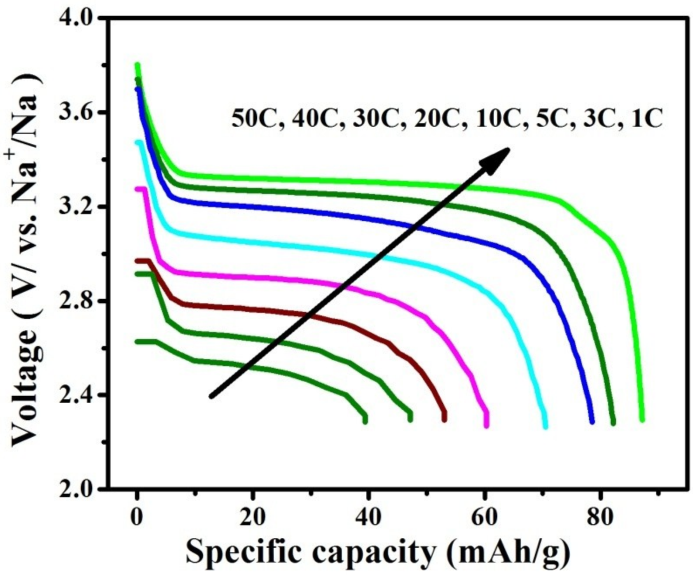

Fig. S10 Discharge curves of NVP@C electrode.

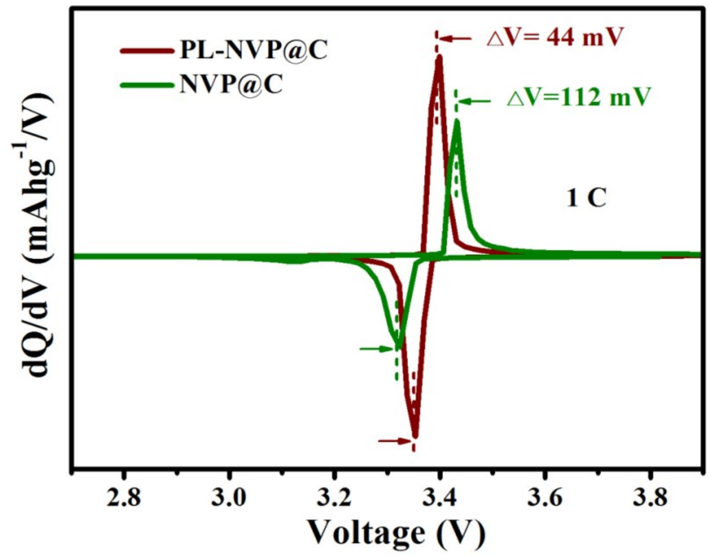

Fig. S11 dQ/dV curves of PL-NVP@C and NVP@C samples.

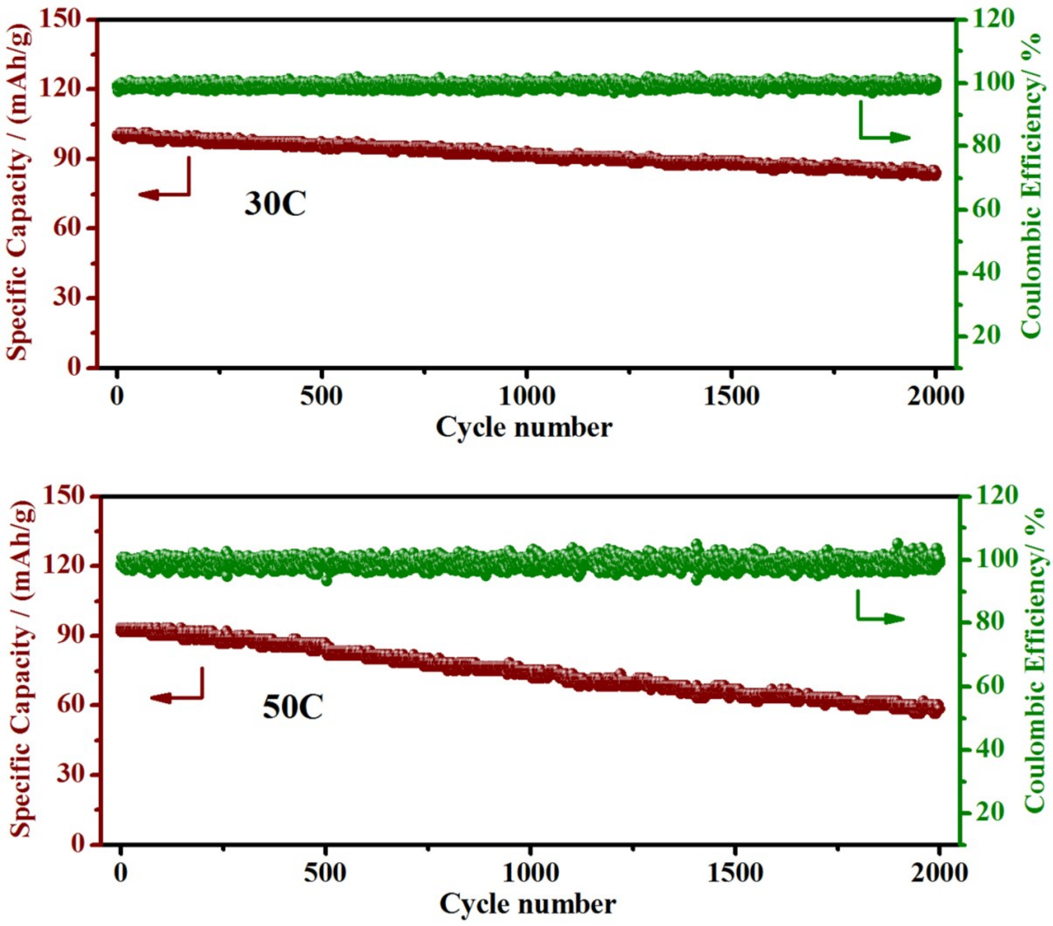

Fig. S12 Cycling performances of PL-NVP@ for over 2000 cycles

at (a) 30C and (b) 50C, respectively.

Table S2 Kinetic parameters of PL-NVP@C and NVP@C obtained from EIS equivalent circuit fitting.

Samples	R_e (Ω)	R_{ct} (Ω)	Diffusion coefficient D_{Na+} (cm^2/s)
PL-NVP@C	4.69	56.84	8.33×10^{-13}
NVP@C	3.89	151.2	4.65×10^{-14}

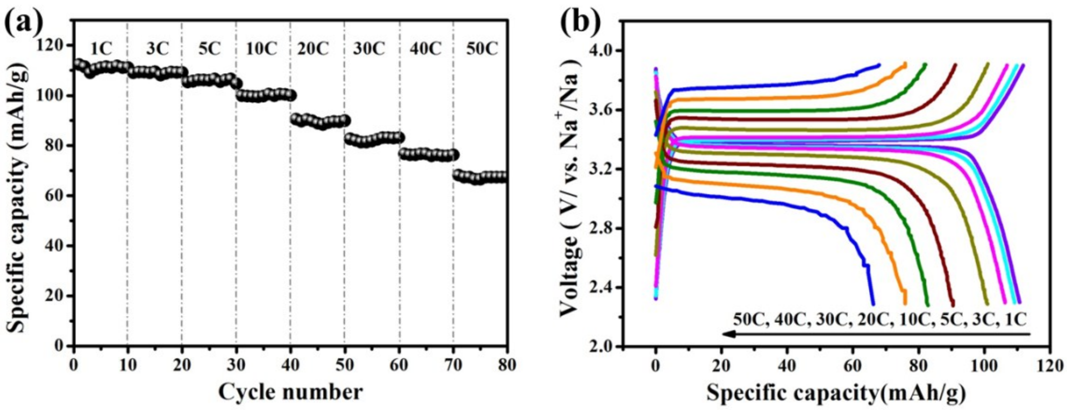

Fig. S13 (a) Rate performance and (b) charge/discharge curves of PL-NVP@C from 1 to 50C (charged and discharged under same rates).

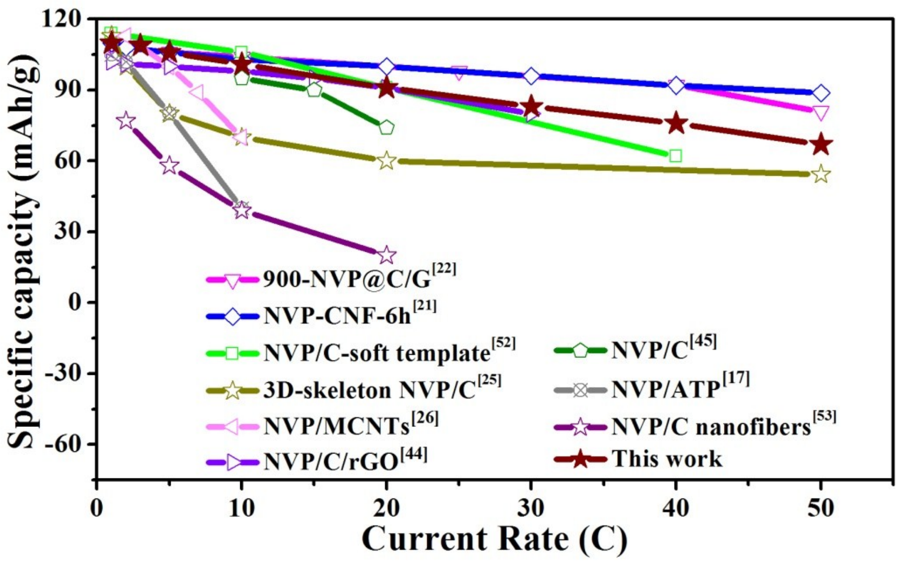

Fig.S14 Comparison of the rate capabilities of PL-NVP@C with other NVP@C materials reported before (charged and discharged under same rates).

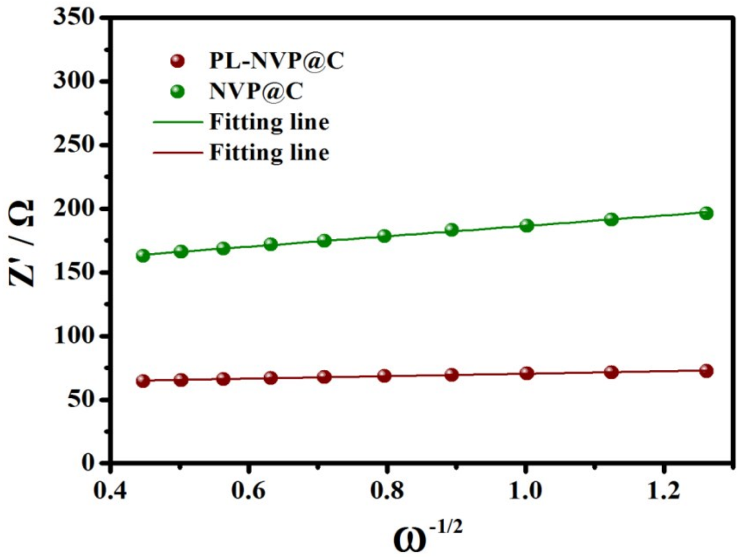

Fig. S15 The relationship between Z_{re} and $\omega^{-1/2}$ in the low frequency region.